

# HOMOGENEITY ANALYSIS OF HIGH YIELD MANUFACTURING PROCESS OF MEMS-BASED PZT THICK FILM VIBRATIONAL ENERGY HARVESTERS

A. Lei<sup>1\*</sup>, R. Xu<sup>1</sup>, C.M. Pedersen<sup>1</sup>, M. Guizzetti<sup>2</sup>, K. Hansen<sup>2</sup>, E.V. Thomsen<sup>1</sup> and K. Birkelund<sup>1</sup>

<sup>1</sup>Department of Micro- and Nanotechnology, Technical University of Denmark

<sup>2</sup>Meggitt Sensing Systems, Denmark

\*Presenting Author: Anders.Lei@nanotech.dtu.dk

**Abstract:** This work presents a high yield wafer scale fabrication of MEMS-based unimorph silicon/PZT thick film vibrational energy harvesters aimed towards vibration sources with peak frequencies in the range of a few hundred Hz. By combining KOH etching with mechanical front side protection, SOI wafer to accurately define the thickness of the silicon part of the harvester and a silicon compatible PZT thick film screen-printing technique, we are able to fabricate energy harvesters on wafer scale with a yield higher than 90%. The characterization of the fabricated harvesters is focused towards the full wafer/mass-production aspect; hence the analysis of uniformity in harvested power and resonant frequency.

**Keywords:** MEMS, Energy harvester, High yield, Screen printing, PZT thick film

## INTRODUCTION

With the recent development in low power electronics and small-scale energy harvesters, the realization of small long-term autonomous wireless sensors seems to become increasingly realistic. Vibrational harvesting of excess mechanical energy using piezoelectric transducers have gained much attention due to high coupling efficiency and simple design [1], but a major issue is the opposite relationship between size of the energy harvester and the frequency of the vibration source. The criterion for success for energy harvesters is that their size does not exceed the volume batteries would take up to supply the required power in the sensors lifetime. This can be well achieved using MEMS technology, however most applicable vibration sources have peak frequencies in the range of a few hundred Hz [2] which for classical MEMS devices are considered unusually low. Nevertheless, several MEMS technology based vibrational harvesting devices with resonant frequencies aimed for this frequency range have been presented [3], [4]. To achieve these resonant frequencies, designs with high length to thickness ratios and relative large proof masses have been utilized, resulting in devices that are laterally large and fragile during the fabrication processes.

Recently Lei et al. [5] presented a high performance MEMS-based PZT thick film unimorph vibrational energy harvester aimed towards a resonant frequency around 200 Hz. The harvester devices, each consisting of a cantilever design with a  $1 \times 1 \text{ cm}^2$  footprint, are fabricated using standard silicon MEMS processes with a yield around or higher than 90%. The high yield is mainly achieved by the use of KOH etching with a mechanical front side protection for cantilever definition in combination, with a SOI wafer for accurately control of the silicon thickness. The active PZT layer is deposited on the silicon cantilever using a silicon compatible PZT thick film screen-printing technique. In [5], and as for a majority of

other MEMS-based vibrational energy harvesters reported, only measurements for a single device is presented. Based on an identical fabrication process as in [5], characterization of each device from a full wafer will be presented in this paper hence, giving a comprehensive assessment of the device uniformity for the high yield wafer fabrication of vibrational PZT thick film energy harvesters.

## FABRICATION

The unimorph vibrational energy harvester is fabricated using a five mask fabrication process on a 4 inch SOI wafer with a  $20 \text{ }\mu\text{m}$  device layer, a  $1 \text{ }\mu\text{m}$  buried oxide layer and a  $500 \text{ }\mu\text{m}$  thick substrate (Fig. 1(a)). A  $1 \text{ }\mu\text{m}$   $\text{SiO}_2$  layer is thermally grown followed by a deposition of  $170 \text{ nm}$  stoichiometric LPCVD silicon nitride (Fig. 1(b)). Backside openings in the silicon nitride for the KOH etch are defined using UV lithography followed by RIE etching and the front side nitride is removed in a RIE etch (Fig. 1(c)). A bottom electrode consisting of a  $50 \text{ nm}$  titanium adhesion layer and a  $500 \text{ nm}$  platinum layer, also serving as a diffusion barrier [6], is deposited using e-beam deposition. The bottom electrode is patterned using UV lithography followed by a wet etch in  $\text{H}_2\text{O}:\text{HCl}:\text{HNO}_3$  (8:7:1) at an elevated temperature (Fig. 1(d)). On top of the bottom electrode a  $27 \text{ }\mu\text{m}$  PZT thick film is deposited using screen printing (Fig. 1(e)). Before the sintering, the PZT thick film is high pressure treated [7]. As top electrode, a  $400 \text{ nm}$  gold layer is deposited by e-beam evaporation through a shadow mask (Fig. 1(f)). The front side of the wafer is protected using a mechanical holder while the  $\text{SiO}_2$  is removed in bHF and the cavities are etched in KOH, with the buried oxide functioning as an etch stop layer (Fig. 1(g)). The PZT structures are covered with resist and the cantilevers are released by a  $\text{SiO}_2$  etch in bHF followed by a silicon etch using RIE (Fig. 1(h)). The PZT thick film is polarized by applying an electric field between the top and bottom electrodes.

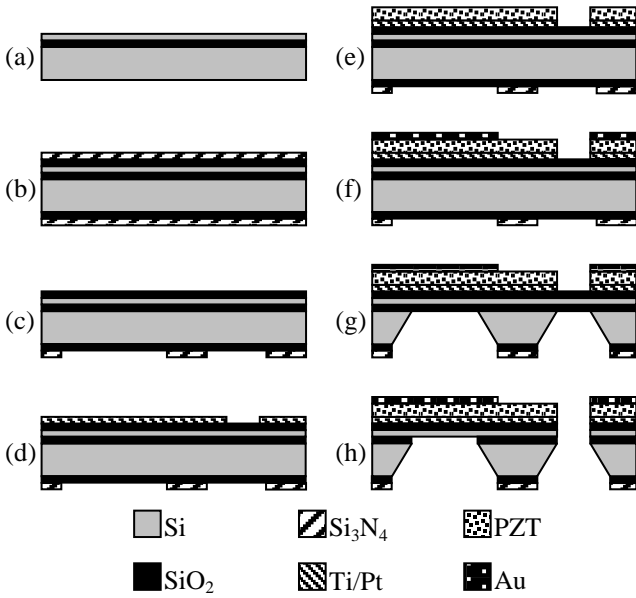


Fig. 1: Process flow for the unimorph MEMS-based PZT thick film vibrational energy harvester.

### Fabrication Yield

The fabricated wafer accommodates 45 harvester devices with the dimensions listed in Table 1. The layout consists of 5 rows with 7 harvester devices and 2 rows with 5 harvester devices. A total of four chips were lost resulting in a yield of ~91 %. Fig. 2 shows a photography of the front and backside of two harvester devices.

Table 1: Dimensions of the energy harvesters.

Frame dimensions	10 mm × 10 mm
Medial dimension	< 1 mm
Cantilever width	5.5 mm
Cantilever length	3.25 mm
Mass width	5.5 mm
Mass length	3.25 mm

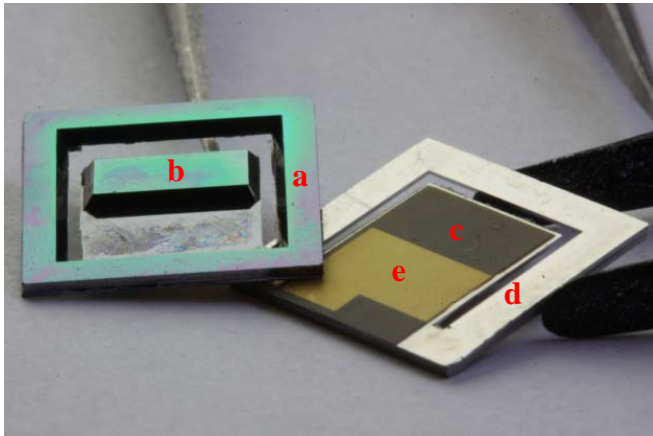


Fig. 2: Photograph showing front and back side of the fabricated energy harvesting devices. (a) frame, (b) proof mass, (c) PZT thick film, (d) bottom electrode and (e) top electrode.

## CHARACTERIZATION

The characterization of the harvesters is carried out in the following way: initially, the capacitance together with open circuit voltage ( $V_{oc}$ ) and resonant frequency ( $F_{res}$ ) is measured for all harvesters. Secondly, the power output dissipated in a resistive load is measured for a number of representative chips.

For the initial part, the capacitance is measured using a HP 4278A capacitance meter, and the open circuit voltage and resonant frequency are measured by vibrating the harvesters using a TIRA TV51110 shaker driven by a sinusoidal signal from an Agilent 33250A function generator. The excitation acceleration is measured using a PCB Piezotronics 301A11 accelerometer with a PCB Piezotronics 482A23 sensor signal conditioner. The acceleration is measured as RMS values in fractions of the gravitational acceleration  $g$  ( $9.81 \text{ m s}^{-2}$ ). For the power output analysis, the harvester is connected to a resistive load and the power output, measured as RMS value, is calculated using  $P = V_{rms}^2 / R_{Load}$ . The resistive load providing optimal power output is found by iteratively changing the resistance of the load.

## RESULTS

The measured capacitances for the 41 fabricated harvesters listed as the wafer layout with rows and columns is seen Table 2. The average measured capacitance is 5.638 nF with a sample standard variation of 0.246 nF. The average capacitance corresponds to a dielectric constant of 842.

Table 2: Measured capacitance in nF for the 41 fabricated harvesters.

	A	B	C	D	E	F	G	[nF]
1		5.342	5.448	5.495	5.234	5.096		6 5.64 5
2	5.336	5.640	5.693	5.679	5.600	5.506	5.343	
3	5.139		5.799	5.769	5.636	5.564	5.398	
4	5.768	5.766	5.839	5.924		5.724	5.004	
5	5.789	5.868	5.884	5.924	5.934	5.896	5.449	
6	5.765	5.958	5.671		5.779	5.615	5.588	
7			5.812	5.853	5.749	5.869		

Table 3: Measured RMS open circuit voltage for the 41 harvesters at resonance with an input RMS acceleration of 0.5 g.

	A	B	C	D	E	F	G	[V]
1		0.75	1.06	0.985	1.30	0.507		2.7 1.6 0.5
2	1.173	0.96	1.21	1.32	1.52	1.07	1.88	
3	2.40		1.08	1.41	1.07	1.27	2.08	
4	2.09	2.15	2.25	1.31		1.72	1.10	
5	2.27	2.20	1.84	1.00	1.28	1.60	2.41	
6	2.70	2.07	2.11		1.55	1.99	1.83	
7			2.10	1.53	1.77	1.79		

The RMS  $V_{oc}$  for the fabricated harvesters measured at resonance with an input RMS acceleration of 0.5 g is listed in Table 3. The average  $V_{oc}$  is 1.6 V with a sample standard variation of 0.52 V. The resonant frequency at which maximum  $V_{oc}$  is obtained is listed in Table 4. The average  $F_{res}$  is measured to 333.3 Hz with a sample standard deviation of 9.9 Hz.

Table 4: Resonant frequencies determined simultaneously with the maximum open circuit voltage. Measurements performed with an input RMS acceleration of 0.5 g.

	A	B	C	D	E	F	G	[Hz]
1		298.2	331.4	323.9	322.6	341		350.1
2	316	336.8	344.3	331.9	343	330.5	342.8	
3	335.5		323	326.9	335.1	333.2	344.1	
4	332.4	339.5	339.7	326.6		343.8	327	333.3
5	331.8	338.5	334.6	318.3	322.9	330	347.2	
6	328	325.5	340.7		334.9	346.8	350.1	
7			337.2	334.5	341	334.5		298.2

### Load Measurements

For the power output measurements a total of 10 representative harvester devices are selected. Three devices are selected from around each of the three quartiles ( $Q_1=1.17$  V,  $Q_2=1.55$  V and  $Q_3=2.08$  V) of the open circuit measurements, the last harvesters selected is the one with highest  $V_{oc}$  output. In Table 5 the iteratively found optimal resistive load is listed for each of the selected harvesters together with the measured RMS power output for the three RMS accelerations 0.5 g, 0.75 g and 1 g. The listed bandwidth is measured as full width at half maximum ( $BW_{FWHM}$ ) at 0.5 g acceleration and the total quality factor is calculated as  $Q_{total}=F_{res}/BW_{FWHM}$ . In Fig. 3 the results are outlined with power output at the three accelerations plotted for each of the 10 harvesters.

Table 5: RMS power output measurements for 10 harvester devices representative for the 41 fabricated devices. Power is measured at three different RMS accelerations with the resistive load listed. Bandwidth ( $BW_{FWHM}$ ) and total quality factor ( $Q_{total}$ ) is measured at 0.5 g.

	Chip	Load [k $\Omega$ ]	$BW_{FWHM}$ [Hz]	$Q_{total}$	RMS Power [ $\mu$ W]		
					0.5 g	0.75 g	1 g
Peak	A6	150	5.00	65.9	12.5	25.0	39.3
Q3 2.08V	G3	50	6.80	50.7	10.5	22.1	35.0
	B4	50	6.80	49.7	9.6	21.3	35.8
	B6	50	6.60	49.3	9.7	21.4	34.7
Q2 1.55V	F5	50	8.20	40.1	6.7	15.7	25.7
	D7	75	9.00	37.1	6.1	14.8	24.3
	E6	75	8.50	39.2	5.5	13.1	22.5
Q1 1.17V	C2	75	8.75	37.7	4.8	11.1	17.9
	A2	75	8.20	38.4	5.1	10.9	15.3
	C3	75	10.25	31.1	2.9	7.2	13.3

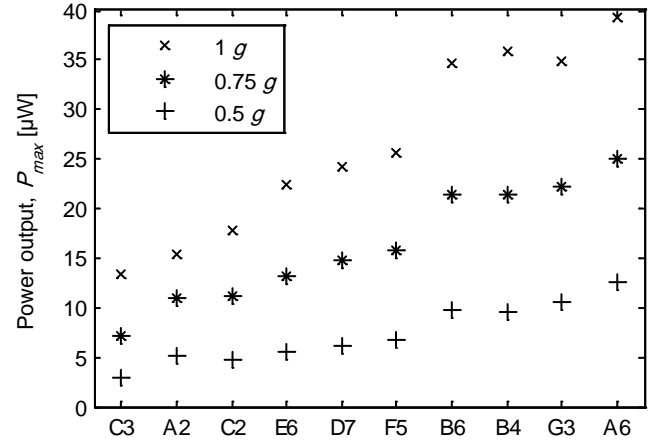


Fig. 3: Measured RMS power output for three different accelerations plotted for the 10 representative harvesters.

## DISCUSSION

Assuming that the porosity and thus the dielectric constant of the screen-printed PZT thick film is constant over the wafer, the measured variation in capacitance is an estimate of geometrical variations. The lateral dimensions of the capacitor are defined by the deposited electrodes which are controlled by lithography. It can therefore be assumed that the main contribution to the variation in capacitance is variations in thickness of the PZT thick film. Percentagewise the sample standard deviation is 4.4% relative to the average value. This corresponds to a variation of 1.2  $\mu$ m out of a PZT film thickness of 27  $\mu$ m. Ignoring the three lowest measured capacitances, this value decreased to 0.9  $\mu$ m.

From an application point of view the main success criteria for a linear vibrational energy harvester is the frequency match with the vibration source. The resonant frequency is determined by mechanical properties with the cantilever thickness and distance from cantilever anchoring point to center of mass as the dominating geometrical parameters. The silicon part of the cantilever is determined accurately by the SOI wafer and the capacitance measurements indicated a relatively small thickness variation of the PZT thick film. The distance to the center of mass, width of the cantilever and mass of the proof mass are all determined by lithography. The sample standard deviation relative to the average measured  $F_{res}$  is 3.0 %, ignoring the two lowest and highest measurements this value decreases to 2.2 %. Since  $F_{res}$  is proportional to the square root of the cantilever thickness cubed, the relative variation is expected to be higher although the silicon part accounts for a high part of the cantilever stiffness. This could indicate that the variation in capacitance across the wafer is caused by both varying dielectric constants and PZT thicknesses.

While the capacitance and  $F_{res}$  measurements give estimates of the variation of the mechanical parameters and the dielectric constant, the open circuit voltage measurements will provide information concerning variations in piezoelectric coefficients and quality

factor since  $V_{oc}=g_{31}\bar{\sigma}h_{PZT}$ , where  $g_{31}$  is the piezoelectric voltage coefficient,  $\bar{\sigma}$  is the average induced stress in the PZT layer with thickness  $h_{PZT}$ . Besides being determined by mechanical properties, which also affects the resonant frequency, the average induced stress is related to the tip displacement at resonance and thus quality factor. The measured sample standard deviation relative to the average  $V_{oc}$  is 32.6 %, ignoring the two lowest and highest values gives a percentage of 27.8 % which is still higher than what the variation in PZT thickness can account for. The majority of the variation in  $V_{oc}$  is therefore believed to originate from either  $g_{31}$  which is determined by how well the PZT thick film is polarized or the quality factor.

Except from the  $V_{oc}$  measurements where the harvesters from the lower left corner of the wafer appears to have a general higher output, no significant wafer area tendencies are observed in the capacitance and  $F_{res}$  measurements nor in-between all three measurements.

For the output power measurements the best uniformity in performance is observed in-between the three chips from the third quartile. The difference in power output is around or less than 1  $\mu$ W for the three accelerations. Similar small variations are observed in bandwidth and total quality factor. The resonant frequency varies from 325-344 Hz for the three chips which is considerably more than the measured bandwidth of around 6.8 Hz. The variation in power output of the three chips from the second quartile increases to around 3  $\mu$ W difference at 1 g. For the first quartile chips, the variation is around 4.5  $\mu$ W at 1 g. In average the first quartile devices harvest 30 % and 36 % less power than the second quartile devices at 0.5 g and 1 g, respectively. Third quartile devices perform 63 % and 45 % better than second quartile devices at 0.5 g and 1 g, respectively. Compared to the variation of the open circuit measurements this increased variation is expected since the output power is proportional to the voltage squared. The relationship between increasing quality factor and increasing power output indicates that the main cause of variation in performance is variation in quality factor and not piezoelectric coefficients.

## CONCLUSION

Using a silicon-based fabrication process involving SOI wafers, KOH etching and screen-printing of PZT thick film, a yield of 41 out of 45 (~91 %) harvester devices for a wafer was achieved. Measurements of the open circuit voltage for the 41 devices showed a relative difference of 32.6 % between the standard deviation and average. Measurements of the capacitance and resonant frequency showed a relative difference between the standard deviation and average value of 4.4 % and 3 % respectively. This indicates that the main variation in open circuit voltage

performance is caused by varying quality factor.

Output power measurements using an optimized resistive load, showed good uniformity between chips with similar open circuit voltages from the high performance section. Decreasing uniformity was observed between chips from the less good performing sections of the open circuit voltage measurements. A maximum power output of 39.3  $\mu$ W was measured at 1 g for the best performing harvester. The power harvesting bandwidth was measured to 5-10 Hz, with the best performing harvesters having the lowest bandwidth. The average resonant frequency was measured to 333 Hz with a standard variation of 9.9 Hz. From an application point of view, either the bandwidth should be increased to cover the variation in resonance, or the variation of the resonant frequency must be decreased.

## REFERENCES

- [1] Beeby S P, Tudor M J, White N M 2006 Energy harvesting vibration sources for microsystems applications *Meas. Sci. Technol.* **17** R175–95
- [2] Roundy S, Wright P K, Rabaey J 2003 A study of low level vibrations as a power source for wireless sensor nodes *Computer Communications* **26** 1131–44
- [3] Elfrink R, Kamel T M, Goedbloed M, Matova S, Hohlfeld D, van Andel Y, van Schaijk R 2009 Vibration energy harvesting with aluminum nitride-based piezoelectric devices *J. Micromech. Microeng.* **19** 094005
- [4] Shen D, Park J-H, Noh J H, Choe S-Y, Kim S-H, Wickle III H C, Kim D-J 2009 Micromachined PZT cantilever based on SOI structure for low frequency vibration energy harvesting *Sensors and Actuators A: Physical* **154** 103–8
- [5] Lei A, Xu R, Thyssen A, Stoot A C, Christiansen T L, Hansen K, Lou-Møller R, Thomsen E V, Birkelund K 2011 MEMS-based thick film PZT vibrational energy harvester *Proceedings, IEEE micro electro mechanical systems* 125–8
- [6] Hindrichsen C C, Pedersen T, Thomsen E V, Hansen K, Lou-Møller R 2008 Investigation of Top/Bottom Electrode and Diffusion Barrier Layer for PZT Thick Film MEMS Sensors *GFER* **367** 201–13
- [7] Hindrichsen C G, Lou-Møller R, Hansen K, Thomsen E V 2010 Advantages of PZT thick film for MEMS sensors *Sensors and Actuators A: Physical* **163** 9–14